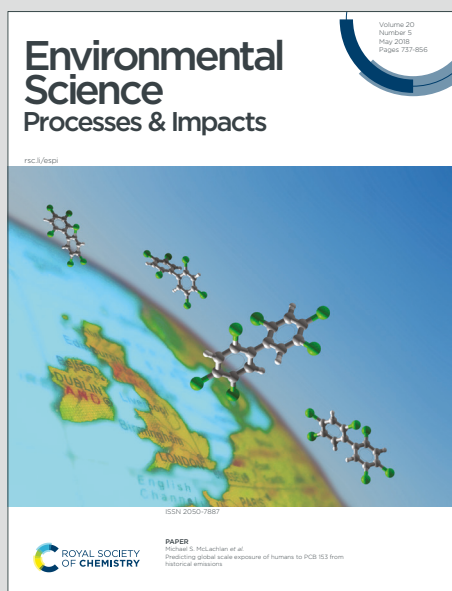


# Environmental Science Processes & Impacts

Accepted Manuscript

This article can be cited before page numbers have been issued, to do this please use: N. Pokhrel and H. Foroutan, *Environ. Sci.: Processes Impacts*, 2026, DOI: 10.1039/D5EM00876J.



This is an Accepted Manuscript, which has been through the Royal Society of Chemistry peer review process and has been accepted for publication.

Accepted Manuscripts are published online shortly after acceptance, before technical editing, formatting and proof reading. Using this free service, authors can make their results available to the community, in citable form, before we publish the edited article. We will replace this Accepted Manuscript with the edited and formatted Advance Article as soon as it is available.

You can find more information about Accepted Manuscripts in the [Information for Authors](#).

Please note that technical editing may introduce minor changes to the text and/or graphics, which may alter content. The journal's standard [Terms & Conditions](#) and the [Ethical guidelines](#) still apply. In no event shall the Royal Society of Chemistry be held responsible for any errors or omissions in this Accepted Manuscript or any consequences arising from the use of any information it contains.

1  
2  
3  
4  
5  
6  
7  
8  
9  
10  
11  
12  
13  
14  
15  
16  
17  
18  
19  
20  
21  
22  
23  
24  
25  
26  
27  
28  
29  
30  
31  
32  
33  
34  
35  
36  
37  
38  
39  
40  
41  
42  
43  
44  
45  
46  
47  
48  
49  
50  
51  
52  
53  
54  
55  
56  
57  
58  
59  
60

Microplastics (MPs) can be transported from oceans to the atmosphere via film and jet droplets released during bursting bubbles, but the role of their surface properties in this process remains poorly understood. Our study demonstrates that MP wettability influences their concentration in airborne droplets—but this effect is pathway-specific. Hydrophobic MPs transfer more efficiently via jet drops, while no clear effect was observed for film drops, suggesting more complex mechanisms at play. These findings offer insights into how MPs may contribute to atmospheric pollution, cloud formation, and long-range contaminant transport. By emphasizing the role of MP surface properties, this work underscores the need for further laboratory studies to refine MP enrichment models and improve understanding of plastic pollution transport and fate.

Downloaded on 12/24/2025 2:42:33 PM  
This article is licensed under a Creative Commons Attribution-NonCommercial 3.0 Unported Licence.



## Journal Name

## ARTICLE TYPE

Cite this: DOI: 00.0000/xxxxxxxxxx

Effect of wettability on microplastics aerosolization via film and jet drops ejected from bursting bubbles<sup>†</sup>Nishan Pokhrel<sup>a</sup> and Hosein Foroutan<sup>a\*</sup>

Received Date

Accepted Date

DOI: 00.0000/xxxxxxxxxx

Bubble bursting during oceanic breaking waves releases tiny droplets that can transport species—including sea salt, microorganisms, and microplastics—across the air-water interface. While many studies have investigated particle-bubble interactions and the role of particle wettability on the particle attachment to rising bubbles, a limited number have extended this to particle aerosolization onto the ejected droplets. This study aims to experimentally investigate how wettability of microplastic (MP) particles affects their aerosolization via the two major droplet ejection pathways from a bursting bubble: film and jet drops. Controlled experiments are conducted with 1  $\mu\text{m}$  diameter surface-modified polystyrene MPs of two contrasting wettabilities (i.e., hydrophilic vs. hydrophobic) in ultrapure water. Film and jet drop pathways are isolated by generating two distinct bubble populations known to primarily produce each droplet type. Results show that the aerosolization factor – defined here as the air-to-water MP concentration ratio – of hydrophobic MPs is approximately one order of magnitude higher than that of hydrophilic MPs for jet drops. In contrast, no significant difference was observed for the film drop aerosolization factor, which can be attributed to a potentially complex effect that MP particles can have on bubble film stability, bursting, and enrichment dynamics. These findings highlight that MP surface properties can significantly influence their ejection into the atmosphere at the ocean surface. Given the potential for inhalation and long-range transport, this mechanism may contribute to the global dispersion of airborne MP pollutants. The results underscore the need to consider aerosolization pathways in the environmental fate and risk assessment of plastic pollution.

## Introduction

Bubble bursting during oceanic breaking waves is a crucial component of the ocean-atmosphere interaction. These bursting bubbles release sea spray aerosol (SSA) that can transport species, including sea salts, bacteria, viruses, dissolved gases, and organic matter across the air-water interface<sup>1–4</sup>. Microplastics (MPs) have been similarly observed to transfer across the air-water interface via bubble bursting<sup>5–8</sup>. MPs, an emerging critical environmental pollutant, have been observed in every environmental compartment on Earth<sup>9</sup>, including marine environments<sup>10</sup>, soil<sup>11</sup>, freshwater systems<sup>12,13</sup>, and the atmosphere<sup>5,14</sup>. Recent studies have considered oceans to be one of the major sources of atmospheric MPs<sup>15</sup>. Atmospheric MP is an emerging air pollutant, with potential health risks to living beings<sup>16–19</sup>, and can be a vector for a wide range of toxic pollutants<sup>20</sup>. Therefore, it is critical to constrain the oceanic source of atmospheric MPs. Physical understanding of the processes involved in (and affecting) the

ocean-to-atmosphere transfer of MPs is a crucial step to constrain the ocean source<sup>21</sup>.

During breaking waves, large volumes of air enter the water and rise up in the form of bubbles that burst at the surface releasing SSA via the two major droplet ejection pathways: film and jet drops<sup>22</sup>. Shattering of the surface bubble cap releases hundreds of film drops, while the collapse of the resulting cavity emits a series of jet drops vertically upwards. Due to differences in ejection mechanisms, film drops are generally in the sub-micron size range ( $< 1\mu\text{m}$ ), while jet drops are generally in the super-micron range<sup>2,3,23</sup>. Bubbles rising up in MP-contaminated waters can scavenge MPs, enriching them at the bubble interface, which are eventually aerosolized via film and jet droplets<sup>24</sup>. It is well-known that contaminant species can be present in substantially higher concentration in the resulting droplets compared to that in the bulk water, thus amplifying the influence of those contaminants<sup>4,25,26</sup>. Additionally, water and particle properties can potentially affect the process of MP scavenging and the resulting enrichment onto droplets.

MPs are generally considered to be hydrophobic, but environmental factors such as heat, ultraviolet (UV) radiation<sup>27</sup>, mechanical forces, biofouling<sup>28</sup>, absorption of organics and chem-

<sup>a</sup> Department of Civil and Environmental Engineering, Virginia Tech, Blacksburg, Virginia 24061, USA.

\* Corresponding author (E-mail: hosein@vt.edu)

icals like PFAS<sup>29</sup> are known to significantly affect surface chemistry and/or wettability of MPs<sup>9,30</sup>. Photo-oxidation is the major route for polymer degradation in the environment<sup>31,32</sup>, and Al Harraq *et al.*<sup>32</sup> observed that the UVA-weathered polyethylene (PE) exhibited increased wettability and dispersibility in the water. Such dynamic changes in wettability present a challenge in predicting the fate of microplastics in the environment<sup>27</sup>. Additionally, once airborne, MPs bearing hydrophilic groups can potentially act as condensation nuclei of cloud ice and water, highlighting the role of MP wettability on cloud formation processes<sup>33–35</sup>. These studies underscore the importance of addressing the role that particle wettability plays in the process of water-to-air transfer of MPs.

Many laboratory studies have investigated the aerosolization of MP particles via single bubbles as well as some developed theoretical models for film and/or jet drop enrichment<sup>8,25,36,37</sup>. Other laboratory studies have used a number of bubble generation mechanisms, typically to “model” oceanic wave breaking processes<sup>6,7,38–41</sup>. These studies have generally focused on the role of (i) MP properties (polymer type, size, concentration, density, surface composition), (ii) bubble properties (size), and (iii) water properties/composition (salinity, surfactant, organic matters) on the transfer of MP at the air-water interface.

Despite that, limited laboratory studies have attempted to address the uncertainties surrounding the effect of the surface properties of MP on their selective enrichment onto film and jet drops<sup>24,42</sup>. It is well-known that particle hydrophobicity favors selective attachment to rising bubbles<sup>43</sup>. Many studies have investigated particle-bubble interactions<sup>44–47</sup> and the role of particle wettability on the attachment<sup>43,48</sup>, but only a few studies have extended this understanding to particle aerosolization via film and jet droplets ejected by the bubbles<sup>22,42</sup>. Notable studies that have developed particle enrichment models in film<sup>36</sup> or jet drops<sup>8,25,37</sup> based on experiments conducted at the level of a single pure or tap water bubble have not considered the role of particle wettability. Furthermore, these theoretical enrichment models have been applied to estimate MP emission from the oceans via sea spray<sup>8,21</sup>. Early studies in biological aerosols<sup>4,49–51</sup> observed that the hydrophobicity of *Serratia marcescens* bacterial cells enhanced their aerosolization onto the topmost jet droplets. Interestingly, Masry *et al.*<sup>6</sup> observed that the transfer of PE particles increased substantially after they were UV-aged, which is known to reduce hydrophobicity. They attributed this to the increased aggregation of the pristine, more hydrophobic PE at the water’s surface, which lowered their transfer rate. This highlights how complex interfacial behaviors, such as particle aggregation, can govern the net aerosolization rate measured in such laboratory systems<sup>6,7</sup>, and underscores the need for controlled experiments that can systematically isolate the role of wettability from other confounding variables.

Recently, Dubitsky *et al.*<sup>24</sup> used a physics-based theoretical modeling to bound the effects of particle wettability in bubble-mediated MP aerosolization by considering the two extremes of particle hydrophobicity: non-scavenged hydrophilic and fully-scavenged hydrophobic particles – represented by bubble-particle attachment efficiency of 0 or 1, respectively. Their theoretical

modeling results show that perfectly attaching hydrophobic particles can be selectively enriched by several orders of magnitude higher in jet drops compared to film drops, highlighting the key role particle wettability could play in sea-air transport of MPs. Furthermore, they highlight the need for laboratory investigations into the effect of MP properties in order to better inform their theoretical models.

Thus, the primary goal of this study is to conduct a controlled experimental investigation into the effect of microplastic wettability on their aerosolization via film and jet drops emitted via bubble bursting. The approach involves using two types of MPs of atmospherically relevant size that share the same base polymer but have contrasting wettabilities in a multi-bubble bursting setup.

## Materials and Methods

### Film and jet drop production in the SAPT

Based on the experimental setup put forth by Wang *et al.*<sup>52</sup>, a spray aerosol pathway tank (SAPT) was built (Figure 1a) that can generate bubble populations of two distinct size distributions known to produce film and jet drops (Figure 1b)<sup>2,3,22,52,53</sup>. The SAPT comprises three major components: (i) a 30 cm × 30 cm × 60 cm polycarbonate tank; (ii) a glass frit with a pore size 250–500 μm (ROBU® Glasfilter-Geraete GmbH, Hattert, Germany), and (iii) a 10 L pressure vessel connected to the tank with a 0.15 mm diameter orifice (Precision Metal Orifices, O’Keefe, Monroe, CT, USA).

Particle-free air is passed through the glass frit at a rate of 1.4 liters per minute (LPM) into the tank containing 30 L of water producing a plume of coarse bubbles (~ 500 to 1500 μm in radius, see Figure 1b) rising through a height of ~ 30 cm, which upon bursting, *primarily* produce film drops<sup>3,22,52</sup>. Separately, sub-100 μm radius fine bubbles (Figure 1b) were generated by passing pressurized ultrapure water at 60 psi (~414 kPa) through the orifice into the tank. These fine bubble plumes rise ~ 40 cm to the surface and burst to *primarily* produce jet drops<sup>3,22,52</sup>. It is important to note that our use of the term ‘jet drops’ and ‘film drops’ in the context of SAPT refers to droplets ejected by these two distinct bubble populations, acknowledging the potential presence of a mixture – a point expanded in the next section.

### Film and jet droplet size distribution

The size distribution of film and jet droplets generated in the SAPT headspace was measured using a scanning mobility particle sizer (SMPS, Model 3936, TSI, Shoreview, Minnesota, USA) and an aerodynamic particle sizer (APS 3321, TSI, Shoreview, Minnesota, USA). The SMPS, consisting of an Electrostatic Classifier (Model 3080), a Differential Mobility Analyzer (Model 3081), and a Condensation Particle Counter (Model 3025a), measured particles with a mobility diameter ( $D_m$ ) between 14 and 700 nm. The APS measured particles with an aerodynamic diameter ( $D_a$ ) between 0.5 and 20 μm.

For sampling, particle-free air was continuously supplied to the SAPT headspace at 6.1 LPM to flush out aerosols. The concentration of the produced droplets in the headspace was allowed

1  
2  
3  
4  
5  
6  
7  
8  
9  
10  
11  
12  
13  
14  
15  
16  
17  
18  
19  
20  
21  
22  
23  
24  
25  
26  
27  
28  
29  
30  
31  
32  
33  
34  
35  
36  
37  
38  
39  
40  
41  
42  
43  
44  
45  
46  
47  
48  
49  
50  
51  
52  
53  
54  
55  
56  
57  
58  
59  
60

Environmental Science: Processes & Impacts Accepted Manuscript

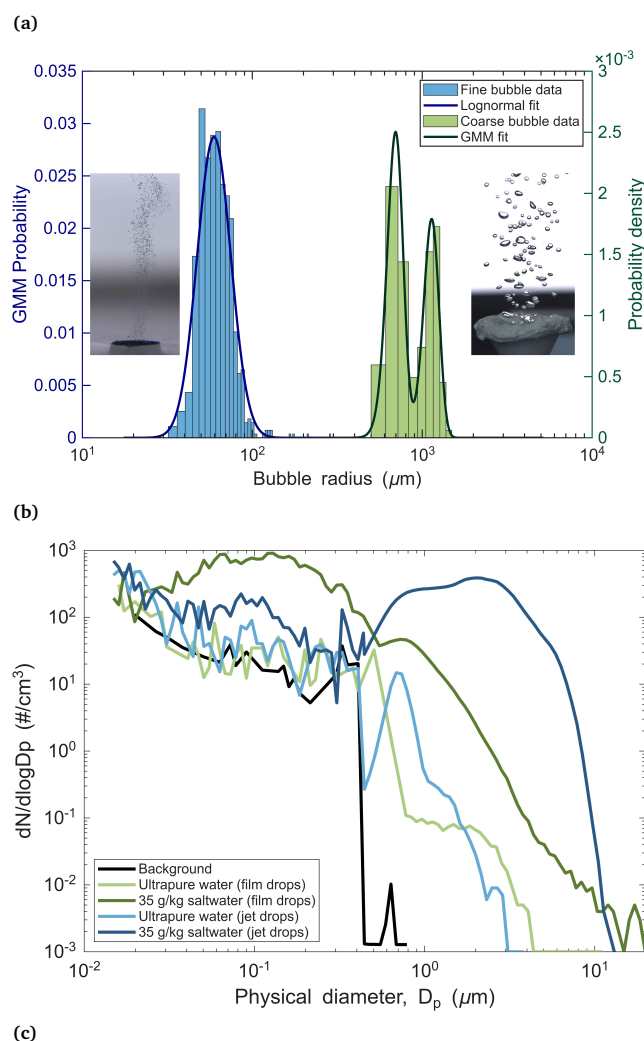
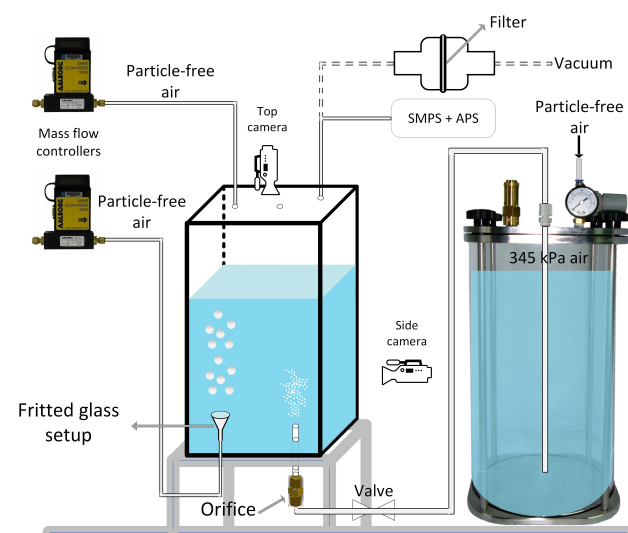


Fig. 1 (a) Schematic of the Spray Aerosol Pathway Tank (SAPT) that consists of a film drop setup producing coarse bubbles of radius between  $\sim 500$  to  $1500 \mu\text{m}$ , and a jet drop setup producing fine bubbles of radius  $< 100 \mu\text{m}$ . (b) Histogram and fitted distribution for fine (blue) and coarse (green) bubbles in the SAPT. Inset shows the photographed sub-surface fine (left inset) and coarse (right inset) bubble plume in the SAPT. (c) Steady-state aerosol size distribution (i) in the background (black), (ii) measured from coarse bubbles bursting in ultrapure (light green) and synthetic seawater (dark green) to produce predominantly film droplets, and (iii) measured from fine bubbles bursting in ultrapure (light blue) and synthetic seawater (dark blue) producing predominantly jet droplets as measured using SMPS and APS without dryer. Synthetic seawater was produced by dissolving sea salt (Instant Ocean Sea Salt, Amazon.com, Inc, Seattle, WA, USA) in ultrapure water ( $\sim 18 \text{M}\Omega\text{cm}$ , Picopure) to achieve a mixing ratio of  $\sim 35 \text{ g kg}^{-1}$ .



to reach a steady state (approximately 5 minutes for film drops and 15 minutes for jet drops). The droplets were then sampled through  $\sim 1$  m of antistatic silicone rubber tubing (McMaster-Carr, Illinois, USA) to the instruments. The SMPS and APS operated in parallel at a scan rate of 5 minutes with sampling flow rates of 0.3 LPM and 1.0 LPM, respectively. All measurements were carried out without a dryer and the relative humidity (RH) was monitored using a HOBO UX100-011 data logger (Onset Computer Corporation, MA, USA) upstream of the aerosol sizing instruments. The RH of the film and jet droplet-laden air stabilized at around 85% before entering the aerosol sizing instruments (Figure S1).

To obtain a single aerosol size distribution spanning the SMPS and APS measurement ranges,  $D_m$  and  $D_a$  size distributions have to be merged (May et al., 2016; Stokes et al., 2013) into a single physical diameter ( $D_p$ ) size distribution. To convert  $D_m$  measured by the SMPS to  $D_p$ , the following relation was used under the assumption of spherical particle geometry:

$$D_m = D_p \quad (1)$$

$D_a$  measured by the APS were converted to  $D_p$  using the following relation:

$$D_p = \frac{D_a}{\sqrt{\frac{\rho_{eff}}{\rho_0}}} \quad (2)$$

where  $\rho_0$  is equal to the unit density ( $1 \text{ g/cm}^3$ ) and  $\rho_{eff}$  is the effective density assigned to the particles sized by the APS. When stitching, particle bins in the overlapping size region of the SMPS and APS were removed due to undercounting of particle concentrations in this size range by both instruments<sup>54</sup>.

The primary experiments in this study were conducted using ultrapure water ( $\sim 18 \text{ M}\Omega \text{ cm}$ , Picopure). However, directly measuring sub-micron film drops (with radii of formation less than  $< 1 \mu\text{m}$ ) produced from ultrapure water is challenging, as they are prone to rapid evaporation and shrinkage as they adjust to the ambient RH within the SMPS. Particles of this size typically equilibrate with their surroundings in about 0.1 seconds or less<sup>3</sup>. To confirm that our SAPT apparatus effectively generates both film and jet drops, we performed a validation experiment using synthetic seawater, which was produced by dissolving sea salt (Instant Ocean Sea Salt, Amazon.com, Inc, Seattle, WA, USA) in ultrapure water to achieve a mixing ratio of  $\sim 35 \text{ gkg}^{-1}$ . Unlike pure water, evaporating saltwater droplets leave behind detectable salt particles.

As shown in Figure 1c, the seawater validation results confirm the presence of a sub-micron mode around  $0.1 \mu\text{m}$  (dark green line), corresponding to film drops that can be attributed to the recently proposed flapping film mechanism for film drop production<sup>55</sup>. This mechanism applies to bubbles in the size range of approximately  $70 - 1200 \mu\text{m}$  in saltwater<sup>23,53</sup>. A recent study by Mazzatenta et al.<sup>53</sup> – which used an intermediate-scale steady state bubble bursting setup to investigate the link between bubbles and emitted droplets – found that the theoretical size scaling and magnitude of the flapping film drops (per Jiang et al.<sup>55</sup>) matched well with their measured droplet size distribution (see

their figure 7). Additionally, we observe a smaller mode around  $1 \mu\text{m}$  that can be attributed to the well-established film centrifuge mechanism for film drop production<sup>56</sup>, applicable to bubbles in the size range of approximately  $900 - 10,000 \mu\text{m}$ <sup>53</sup>.

Similarly, we observe a super-micron mode around  $2 \mu\text{m}$  (dark blue line), which can be attributed to jet drops, as the measured droplet sizes are consistent with theoretical estimates of jet drop size (per Mazzatenta et al.<sup>53</sup>, based on Ganan-Calvo<sup>57</sup>) generated from our fine sub- $100 \mu\text{m}$  bubbles. Additionally, we observe a smaller sub-micron mode around  $0.1 \mu\text{m}$  that can be attributed to flapping film drops produced by the fraction of fine bubbles larger than about  $70 \mu\text{m}$  (per Mazzatenta et al.<sup>53</sup>, based on Jiang et al.<sup>55</sup>), suggesting our setup, as expected, does not exclusively produce film or jet drops.

Consistent with our observations in saltwater, we also observed a mode around  $0.7 \mu\text{m}$  for ultrapure water (light blue line), which can be attributed to jet drops that likely shrank as they adjusted to the ambient RH within the APS. This mode cannot be attributed to film drops, as the bubble sizes responsible for producing  $\sim 1 \mu\text{m}$  film droplets – more precisely, centrifuged film drops – are about  $1\text{--}10 \text{ mm}$  (Mazzatenta et al.<sup>53</sup>, based on Lhuissier and Villermaux<sup>56</sup>), which were not present in our fine bubble setup. On the other hand, a distinct sub-micron mode for film drops – more precisely, flapping film drops – was not resolved, likely due to evaporation. This is consistent with previous reports of limited or no film drop production via bubble bursting in pure distilled water compared to saltwater<sup>3,58</sup>. Similarly, we observed a small super-micron mode around  $2 \mu\text{m}$  that can be attributed to shrunken centrifuged film drops generated via our coarse bubble setup.

### Measurement of sub-surface bubble size distribution

Bubble plumes were photographed from the side of the SAPT using a Nikon D750 DSLR camera (shown in Figure 1a) placed against the backdrop of an LED panel and a precision ruler for scale (Figure S2). Nikon AF-S NIKKOR 24-120mm 1:4 G ED lens was used to photograph coarse bubbles and AF-S VR MICRO NIKKOR 105mm 1:2.8G ED micro-lens was used for fine bubbles. The bubble radius was determined as the projected area radius, defined as the radius of a circle that has an area equal to the projected area of the bubbles. The projected areas were calculated manually from the bubble photographs using the wand tool (with an appropriate tolerance value) in the image processing software ImageJ<sup>59</sup>. Figure 1b left (right) shows the histogram as well as the lognormal (Gaussian mixture model) fit for the fine (coarse) bubbles. Since some coalescence events were observed at the surface (Figure S3), we note that the actual size of certain bubbles just before bursting might be slightly larger but would still tend more toward the film drop production mode.

### Temporal evolution of surface bubbles

Bursting of surface bubbles was recorded from a top-down view against a dark background using a Nikon D750 DSLR camera equipped with an AF-S NIKKOR 24-120mm 1:4 G ED lens (shown in Figure 1a), with bubbles illuminated from the sides by a LED light strip (Figure S4). The recording also captured the display

of the mass flow controller, which regulated airflow through the glass frit. This allowed us to determine the precise moment bubble flow ceased, which was used as the reference time for the experiments. From this reference point, a four-second video segment was extracted for analysis.

To quantify the extent of surface bubbling, we estimated the percentage of the video frame area covered by bubbles. Each frame of the four-second video segment was processed using an ImageJ algorithm that applied a threshold to generate a binary image, separating the white bubbles from the dark background. The fraction of white pixels in each binary frame was used as a proxy for the area occupied by bubbles on the water surface. To ensure consistency across all video samples (15 each), each video was digitally cropped to a uniform region encompassing only the water's surface, correcting for minor variations in camera placement across recordings. This analysis provided a time-resolved estimate of surface bubble coverage, which was used as a proxy for bubble stability and compared across various experiments.

### Microplastics aerosolization experiments

Fluorescent monodisperse 1  $\mu\text{m}$  diameter polystyrene (PS) microspheres of two contrasting wettabilities – hydrophobic sulfate-modified PS (SuPS) and hydrophilic amine-modified PS (AmPS) microspheres (ThermoFisher Scientific, Oregon, USA) – were suspended in ultrapure water ( $\sim 18\text{ M}\Omega\text{ cm}$ , Picopure). This medium was specifically chosen to: (i) eliminate the additional effects of salinity, (ii) establish experimental conditions comparable with previous single-bubble measurements in pure water<sup>8,25,36,60</sup>, and (iii) ensure consistency across all our experimental measurements, including contact angle, zeta potential, and aerosolization. The particle size of 1  $\mu\text{m}$  was selected because it is atmospherically relevant and sufficiently small to be incorporated within both film and jet droplets, rather than excluded due to geometric constraints.

To establish the relative wettability of the two particle types, the apparent contact angle of these microspheres was measured by placing tiny droplets of ultrapure water on a  $\sim 30\text{ }\mu\text{m}$  thick and dry flat surface made up of AmPS and SuPS particles. The flat surface was created by filtering a suspension of those MPs onto a 25 mm polycarbonate filter via a vacuum filter assembly (Sigma-Aldrich®, MO, USA). The droplet had a low contact angle of  $\sim 58^\circ$  on the AmPS layer but a high contact angle of  $\sim 128^\circ$  on the SuPS layer, as measured by a Drop Shape Analyzer (DSA25, Kruss, Germany) (Figure S5). While this measurement provides an apparent value that incorporates surface roughness effects, it serves as a strong proxy for classifying the particles' overall hydrophilic or hydrophobic nature. Additionally, as a measure of surface charge, the zeta potential of SuPS and AmPS suspensions in ultrapure water was measured at a concentration of  $10^{12}$  particles per liter (PPL) using Zetasizer Ultra Red (Malvern Panalytical Ltd., UK) and was found to be  $-57.78\text{ mV}$  and  $-14.54\text{ mV}$ , respectively (Figure S5). Together, these measurements confirm that the two MP types—identical in size and base polymer—differ primarily in surface functionalization. Both are negatively charged, eliminating surface charge sign as a confounding factor, and enabling us to

isolate the role of wettability in modulating aerosolization behavior.

For MP aerosolization via film (jet) drops, three (four) experiments were conducted with ultrapure water at room temperature for each of the SuPS and AmPS suspensions, using a single representative number concentration of  $\sim 10^6\text{ PPL}^{61}$ , as the general effect of particle concentration has already been established in our prior work<sup>62</sup>. Working solutions were prepared by extracting a portion of the manufacturer's stock solution using an Eppendorf pipette, diluted in ultrapure water to achieve the target concentration, stirred, and sonicated for 5 minutes to ensure dispersion of particles. Both SuPS and AmPS were assumed to be well-mixed in the bulk ultrapure water since their density ( $1.055\text{ gcm}^{-3}$ ) was similar to the density of pure water at room temperature ( $1\text{ gcm}^{-3}$ ), resulting in a high settling time on the order of months.

Each MP aerosolization experiment in the SAPT consisted of a 5 minute period of flushing the SAPT headspace with particle-free air, followed by a 5-15 minutes period of bubbling to reach steady-state aerosol concentration in the headspace. This was then followed by a 30-minute (film drop) or 60-minute (jet drop) air sampling period. Air samples – drawn from the tank headspace at a flow rate of 2 LPM – and 20 mL water samples from each experiment were passed through a Polycarbonate Track-Etch (PCTE) membrane filters (Zefon International, FL, USA) using a vacuum filter assembly (Sigma-Aldrich®, MO, USA) to collect MPs for off-line analysis. To capture variations in MP number concentration in water, water samples were taken before and after each experiment. Before starting a new batch of MP experiments, the SAPT was thoroughly cleaned with soap and ultrapure water and disinfected with 70% isopropyl alcohol to eliminate residual contamination from previous experiments.

The air and water PCTE filters were scanned using a fluorescent microscope (EVOS® FL Auto Imaging System, Thermo Fisher Scientific Inc., MA, USA) (Figure S6), and the scanned images were processed using ImageJ<sup>59</sup> to count the number of MPs in the sampled air and bulk water volumes. The aerosolization factor (AF) was defined as the ratio of particle number concentration (PPL) in the sampled volume of air ( $C_a = N_a/V_a$ ) to that in the bulk water ( $C_w = N_w/V_w$ )<sup>7</sup>:

$$AF = \frac{C_a}{C_w} = \frac{N_a/V_a}{N_w/V_w} \quad (3)$$

Here,  $N_a$  represents the total number of aerosolized MPs captured on the PCTE filters during the sampling period, and  $V_a$  denotes the total volume of air drawn from the tank headspace through these filters.  $N_w$  represents the number of MPs present in the volume of water sampled ( $V_w = 20\text{ mL}$ ), assuming a well-mixed condition.

We note that our AF is distinct from the enrichment factor (EF) which is commonly used in single-bubble studies to quantify particle enrichment in droplets<sup>24,25,36</sup>. EF is defined as the ratio of the particle number concentration in the generated film or jet droplets to that in the bulk water. We refrain from estimating EF here due to the significant uncertainties in determining the volume of pure water film or jet droplets produced in our more re-

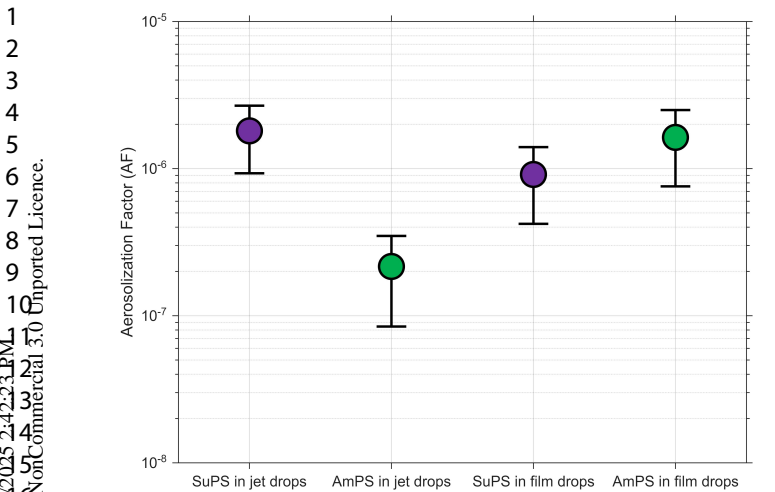


Fig. 2 Experimental aerosolization factors (AF) of 1  $\mu\text{m}$  hydrophobic (SuPS, purple) and hydrophilic (AmPS, green) microplastics in film and jet droplets generated via bursting ultrapure water bubbles in the Spray Aerosol Pathway Tank (SAPT). The aerosolization factor is defined as the ratio of particle number concentration in the sampled air to that in the bulk water. Circular markers represent mean values from replicate experiments ( $n=4$  for jet drops,  $n=3$  for film drops), and the error bars represent  $\pm 1$  standard deviation. The y-axis is on a logarithmic scale.

alistic, multi-bubble bursting setup. Instead, AF offers a more robust metric for comparing aerosolization under these conditions.

## Results and Discussion

### Wettability-Driven Differences in MP Aerosolization

Figure 2 shows the empirical film and jet drop AFs of SuPS (purple) and AmPS (green), with circular markers representing the mean values and error bars representing the standard deviation. Our experimental results show that the jet drop AF of hydrophobic SuPS (mean  $AF_{\text{jet}}^{\text{SuPS}}$  of  $\approx 1.8 \times 10^{-6}$ ) is approximately one order of magnitude higher than that of hydrophilic AmPS (mean  $AF_{\text{jet}}^{\text{AmPS}}$  of  $\approx 2.2 \times 10^{-7}$ ). Interestingly and in contrast, no clear dependence on wettability was observed for aerosolization via film drops: mean AF values of SuPS ( $AF_{\text{film}}^{\text{SuPS}}$ ) and AmPS ( $AF_{\text{film}}^{\text{AmPS}}$ ) in film drops are  $\approx 9.1 \times 10^{-7}$  and  $\approx 1.6 \times 10^{-6}$ , respectively. We acknowledge that the size of the MPs (1  $\mu\text{m}$ ) relative to the predominantly sub-micron film drops imposes a geometric constraint that limits overall aerosolization. Consequently, the observed aerosolization is likely driven by the subset of larger, super-micron ‘centrifuged’ film drops.

The enhanced aerosolization of hydrophobic SuPS in jet drops aligns with the well-established role of particle hydrophobicity in favoring particle-bubble attachment, which subsequently influences particle aerosolization via droplets<sup>24,63</sup>. This finding is also consistent with historical biological aerosol studies, where the hydrophobicity of *Serratia marcescens* bacterial cells enhanced their transfer into the topmost jet droplets produced in distilled water<sup>4,49–51</sup>. On the other hand, Masry *et al.*<sup>6</sup> observed a seemingly opposite trend, where hydrophilic, UV-aged PE aerosolized significantly more than pristine, hydrophobic PE. Given that the bubbles used in their study (supposedly having radii of  $\approx 340 \pm 50 \mu\text{m}$ <sup>6,64</sup>) are of the size known to produce predominantly jet

drops, this discrepancy can be explained by a key difference in the experimental design: they attributed their observation to the formation of aggregates of pristine hydrophobic PE at the water surface which limited the water-to-air transfer rate – an observation consistent with our previous work<sup>7</sup>.

While surface roughness and charge are also known to affect particle-bubble interactions, neither of them explain our observations for the following reasons: (i) the surface morphology was visually observed to be similar between the spherical SuPS and AmPS per images taken using a JEOL IT500 scanning electron microscope (JEOL, Peabody, Massachusetts, USA), and (ii) since bubbles in pure water are negatively charged ( $\sim -35 \text{ mV}$ )<sup>65,66</sup>, the stronger negative charge of SuPS ( $\sim -58 \text{ mV}$ ) should create a greater electrostatic repulsion than for AmPS ( $\sim -15 \text{ mV}$ ), thus hindering attachment. However, the opposite was observed. Therefore, aerosolization differences can be confidently attributed to wettability, indicating that hydrophobic attraction is likely the dominant mechanism.

The lack of a clear wettability effect for film drops, however, suggests a more complex mechanism. It can be assumed that hydrophobic SuPS are more readily scavenged by the bubbles, likely leading to a relatively higher concentration in the bubble cap film. Considering the one order of magnitude difference observed between  $AF_{\text{jet}}^{\text{SuPS}}$  and  $AF_{\text{jet}}^{\text{AmPS}}$ , it is logical to assume a correspondingly higher  $AF_{\text{film}}^{\text{SuPS}}$ . That we do not observe this implies that hydrophobicity does not enhance aerosolization via film drops in the same way, a point we explore further in Section . This difference in AF can be attributed primarily to the difference in the number of SuPS or AmPS emitted via film drops within the sampling duration ( $N_a$ ), since  $V_a$  and  $C_w$  are approximately equal for both cases in eq.(3).  $N_a$  ultimately depends on film drop formation mechanisms that determine the number and size of droplets, which is assumed to be consistent between experiments. Our unexpected result warrants revisiting this assumption.

Studies have shown that the film drop production mechanism is influenced by various environmental factors including temperature, salinity, viscosity, surface tension, and potentially, the presence of insoluble contaminants like micro- and nanoplastic pollution<sup>56,67</sup>. A number of studies – summarized in Table II of Gupta<sup>42</sup> – have found that the presence of particulates in deionized water tends to increase bubble lifetime at the surface. As is well-established, a longer bubble lifetime generally corresponds to a thinner film, as the bubble has more time to drain<sup>67</sup>, which can return a portion of the scavenged MPs back to the bulk water<sup>36</sup>.

The role of particulate wettability in bubble stability and bursting dynamics appears complex. Some studies suggest that hydrophobic particles perforate films and reduce bubble lifetime<sup>68</sup>, while others<sup>69</sup> have found that hydrophobic nanoparticles increase bubble lifetime. Nano-sized particles have been shown to impact surface tension<sup>70</sup> and viscosity<sup>71</sup>, but their observed effects remain inconsistent and contradictory<sup>42,72,73</sup>.



## Surface Bubble Behavior and MP Concentration Effects on Film Drop Emission

Here, we hypothesize that hydrophobic SuPS and hydrophilic AmPS influence the bubble bursting mechanism in different ways by locally altering the surface tension and viscosity of the bubble cap, thus affecting drainage time, film thickness before rupture, and ultimately governing droplet-mediated MP aerosolization<sup>42</sup>.

Therefore, to find preliminary evidence supporting this hypothesis, we conducted two additional sets of complementary, exploratory experiments: one examining how aerosolization varies with MP concentration in water, and another characterizing the temporal evolution of surface bubbles in SuPS- and AmPS-containing solutions.

In the first set, we examined how aerosolization behavior changes with varying MP number concentrations in water. The ratio of  $AF_{\text{film}}^{\text{SuPS}}$  to  $AF_{\text{film}}^{\text{AmPS}}$  shifted accordingly, as shown in Figure 3a. At higher MP concentrations in water, we expect the bubble cap film to contain even more SuPS than AmPS due to bubble scavenging favoring hydrophobic particles. As a result, any differences in how SuPS and AmPS influence film drop production may have become more pronounced at higher MP concentrations—as is indeed the case.

In the second set, we examined the temporal evolution of the surface bubbles following the cessation of active coarse bubble formation in AmPS- and SuPS-containing ultrapure water. Given our limitations in directly measuring bubble thickness and the lifetime of individual bubbles – which came at the expense of our more realistic multi-bubble setup – this set of experiments was designed to provide a general statistical sense of bubble persistence – and, by extension, bubble lifetime and thickness – when AmPS and SuPS are added to ultrapure water. Figure 3b shows how the percentage of the surface area covered by bubbles evolves over the span of four seconds after the cessation of active coarse bubble formation for both AmPS- and SuPS-containing water. The decay in area starts with a delay of approximately 700 ms, which is consistent with the theoretical time required for  $\sim 1$  mm air bubbles to rise approximately 40 cm to the surface. The ratio of these percentages (AmPS to SuPS) – shown in Figure 3c – is mostly greater than one, indicating that bubbles in SuPS-containing ultrapure water dissipated more rapidly. This trend is further reflected in the cumulative decay time scale, defined as the time required for the bubble-covered area to drop below 1% of its initial value. For SuPS, this time was 2314 ms (95% CI: 2140–2489 ms), noticeably shorter than the 3067 ms (95% CI: 2694–3485 ms) observed for AmPS. These results suggest that the surface bubble population in SuPS-containing ultrapure water had a shorter collective persistence, indicating a reduced bubble lifetime. While not exhaustive, these complementary experiments provide indirect evidence consistent with our hypothesis that SuPS and AmPS may have locally altered the fluid properties in different ways, thus affecting the mechanism of MP aerosolization. We emphasize that these results are intended to provide a mechanistic basis for and motivate future detailed investigations into the in-situ dynamics of bubble film rupture and drainage, specifically focusing on how these processes are influenced by micro- and nanosized pollutants<sup>67</sup>.

## Broader Implications and Environmental Relevance

The physical principles of wettability isolated in this study are likely relevant to real-world processes in the ocean, although we acknowledge that the presence of salts, surfactants, and organics in seawater will modulate the magnitude of these enrichment effects. For example, the elevated ionic strength in seawater due to the presence of salts can compress electric double layers around particles and bubbles, thus reducing electrostatic repulsion between them<sup>27,47</sup>. This reduced energy barrier would likely promote attachment even for moderately hydrophilic particles, thus narrowing the contrast between hydrophobic and hydrophilic cases. While wettability likely becomes a weaker discriminating factor during the attachment phase of bubble-particle scavenging (a process involving collision, attachment, and stability<sup>44,47</sup>), it still likely determines the bubble-particle stability efficiency in turbulent ocean conditions<sup>47,74</sup>. At the same time, surface-active materials present in seawater (like fatty acids, proteins, lipids, etc.) can adsorb to particle surfaces thus modifying interfacial properties like wettability and surface charge<sup>25</sup>. With this context in mind, our results provide a basis for speculating on key implications for MP emission from the ocean surface – bearing in mind that such effects will be further influenced by the complex biogeochemistry of natural seawater.

Our findings suggest that hydrophobic MPs are more likely to dominate larger SSA droplets emitted by jet drops – and consequently facilitate the emission of larger MPs (up to 280  $\mu\text{m}$ , as observed by Shaw *et al.*<sup>8</sup>), indicating that wettability may act as a selection mechanism for larger MPs during aerosolization. Hydrophobic MPs can adsorb hydrophobic organic pollutants such as polycyclic aromatic hydrocarbons (PAHs) and polychlorinated biphenyls (PCBs)<sup>75</sup>, suggesting a potential pathway for the long-range atmospheric transport of these pollutants. In contrast, both hydrophilic and hydrophobic MPs can be incorporated into the relatively smaller SSA droplets emitted by film drops. As the estimated 3,400 kilotonnes of floating plastics currently in the ocean<sup>76</sup> undergo further solar degradation – leading to fragmentation and increased wettability – the likelihood of their aerosolization via film drops increases.

While jet drops may contribute more significantly to the total mass of MPs aerosolized in the atmosphere, film drops are known to dominate SSA number concentrations, accounting for 60 to 80 % of the submicrometer SSA fraction<sup>52</sup>. The aerosolization of hydrophilic MPs via smaller film drops may make them more likely to act as cloud condensation nuclei, influencing cloud microphysics and precipitation processes<sup>33–35</sup>. Additionally, hydrophilic MPs could undergo hygroscopic growth, potentially altering their size, optical properties, and atmospheric residence time.

Our identification of particle wettability as a governing factor in aerosolization may help refine estimates of oceanic contributions to atmospheric MPs. According to a recent study by Yang *et al.*<sup>21</sup>, the theoretical upper limit of the global sea-air emission flux of sub-100  $\mu\text{m}$  MPs was estimated to be on the order of  $10^{-2}$  megatons per year, based on current knowledge of oceanic MP concentration, SSA flux, and film and jet drop enrichment models

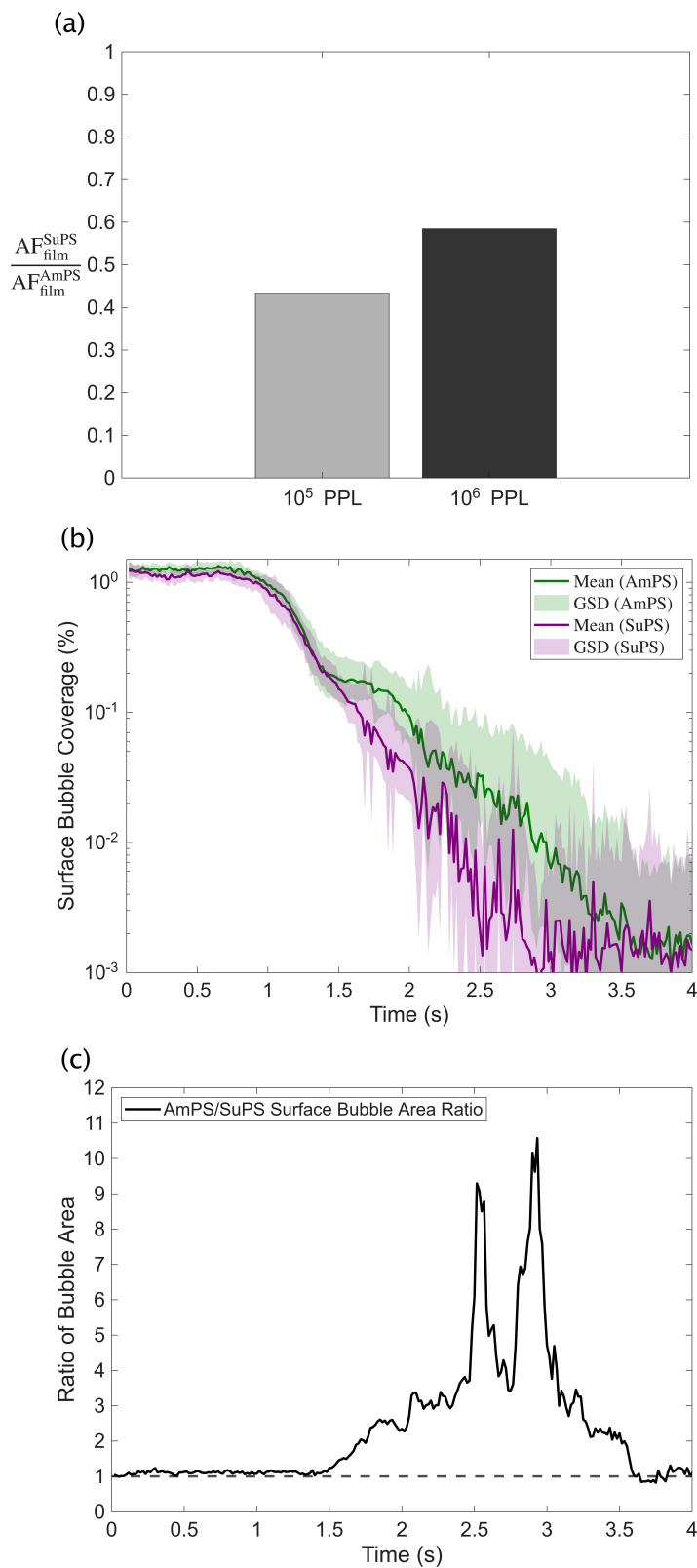


Fig. 3 (a) Ratio of film drop aerosolization factor (AF) for hydrophilic AmPS to hydrophobic SuPS at two MP number concentrations in water. (b) Evolution of the percentage of the tank surface area covered by coarse bubbles over a period of four seconds after the cessation of active bubbling for AmPS- and SuPS-containing ultrapure water (N=15 each). Solid lines represent the geometric mean, and the shaded areas represent  $\pm 1$  geometric standard deviation (GSD). (c) Ratio of the percentage area covered (AmPS to SuPS) shown in (b), highlighting the difference in bubble persistence.

developed by Refs.<sup>25,36,37</sup>). These estimates are based on enrichment models developed in single-bubble bursting experiments in pure or tap water and have not considered MP wettability. Thus, they could change after factoring in the hydrophobicity of micro- and nanosized plastics present in the oceans. As discussed earlier, Dubitsky *et al.*<sup>24</sup> theoretically modeled the effect of MP wettability and estimated that hydrophobic MPs can be selectively enriched by several orders of magnitude higher in jet drops compared to film drops. While their film drop enrichment model does acknowledge the effect of particle size in the film bursting mechanism – by assuming that the particle will initiate bursting when the film thickness approaches the particle size – it does not incorporate the potential impact of particle wettability on bursting dynamics, as our film drop aerosolization and surface bubble area decay results suggests. Additionally, they considered hydrophilic particles to be perfectly non-attaching – granted for the purposes of estimating emission bounds – but we demonstrate that hydrophilic particles do aerosolize via film and jet drops despite the lack of wettability-governed interaction, and thus can have a non-zero attachment efficiency – a metric used to quantify particle wettability in the enrichment models. We note that previous studies have revealed that hydrophilic particles can still exhibit attachment to rising bubbles even without wettability-governed interaction<sup>77,78</sup>.

Incorporating particle wettability into enrichment models could therefore improve the accuracy of MP emission estimates. Future studies employing such refined models will require not only accurate spatial distributions of MPs at the ocean surface but also detailed characterization of their physicochemical properties. Our observations of the absence of a clear effect of MP wettability on aerosolization via film drops, and limited prior work on particle enrichment onto film drops<sup>36,79,80</sup> – compared to numerous studies on jet drops<sup>4,8,25,26,37,81–84</sup> – further highlight the need for improved mechanistic understanding of bubble bursting and drop enrichment dynamics.

Finally, our demonstration of wettability as a key factor in MP aerosolization highlights the importance of future laboratory studies conducted in realistic seawater. Other surface properties – such as surface charge, particle shape, roughness, and biofilm colonization – may also play important roles in enrichment and atmospheric transport<sup>8,42,68</sup>. While some theoretical studies have begun to include these factors – for instance, Ji *et al.*<sup>25</sup> considered particle shape, and<sup>24</sup> incorporated particle wettability – there remains a pressing need for experimental validation under environmentally representative conditions.

## Conclusions

The goal of this study was to conduct a controlled experiment to investigate the effect of particle wettability on aerosolization via film and jet drops. Droplets were attributed to either the film or jet drop pathway based on their generation from two distinct, well-characterized bubble populations known from literature to predominantly produce their respective drop types<sup>53</sup>. To isolate the effect of wettability, we kept constant the properties of the bubbles (fine or coarse), water (ultrapure), and MP (polymer type, size, shape, concentration, density, and surface charge). Our

results demonstrate that wettability of MP particles significantly influences their aerosolization, and does so differently for film and jet drops. The jet drop aerosolization factor of hydrophobic SuPS was approximately one order of magnitude higher than that of hydrophilic AmPS. In contrast, no significant difference was observed in film drop aerosolization factor. We argue that this discrepancy arises from the complex and contradictory effects of particle presence and surface properties on local bubble film behavior, which in turn affect film drop production and particle transfer. Together, our findings highlight the nuanced role of particle surface properties in shaping the aerosolization of microplastics via bubble bursting. These results underscore the importance of interfacial processes in governing microplastic emissions to the atmosphere and motivate continued investigation across different ejection pathways and environmental conditions.

## Author contributions

Nishan Pokhrel: Conceptualization, Data Curation, Formal Analysis, Investigation, Methodology, Visualization, Writing – original draft, Writing – review and editing. Hosein Foroutan: Conceptualization, Formal Analysis, Funding Acquisition, Methodology, Project Administration, Supervision, Validation, Writing – review and editing.

## Data availability

Data used to plot the figures in this article are available at Figshare at <https://doi.org/10.6084/m9.figshare.29906480.v1>.

## Funding

This work is supported by National Science Foundation (NSF) CAREER Award CBET 2145532. The work was performed in shared facilities at the Virginia Tech National Center for Earth and Environmental Nanotechnology Infrastructure (NanoEarth), a member of the National Nanotechnology Coordinated Infrastructure (NNCI), supported by the NSF (ECCS 1542100 and ECCS 2025151).

## Conflicts of interest

There are no conflicts to declare.

## Acknowledgements

The authors thank Dr. William Ducker of Virginia Tech for providing critical insights during the execution of the experiments.

## References

- 1 F. Veron, Ocean Spray, *Annual Review of Fluid Mechanics*, 2015, **47**, 507–538.
- 2 L. Deike, Mass Transfer at the Ocean–Atmosphere Interface: The Role of Wave Breaking, Droplets, and Bubbles, *Annual Review of Fluid Mechanics*, 2022, **54**, 191–224.
- 3 E. R. Lewis and S. E. Schwartz, *Sea Salt Aerosol Production: Mechanisms, Methods, Measurements, and Models - A Critical Review*, American Geophysical Union, 2004.
- 4 D. C. Blanchard, The Ejection of Drops from the Sea and Their Enrichment with Bacteria and Other Materials: A Review, *Estuaries*, 1989, **12**, 127.

5 S. Allen, D. Allen, K. Moss, G. Le Roux, V. R. Phoenix and J. E. Sonke, Examination of the ocean as a source for atmospheric microplastics, *PLoS One*, 2020, **15**, e0232746.

6 M. Masry, S. Rossignol, B. Temime Roussel, D. Bourgoigne, P. O. Bussiere, B. R'Mili and P. Wong-Wah-Chung, Experimental evidence of plastic particles transfer at the water-air interface through bubble bursting, *Environ Pollut*, 2021, **280**, 116949.

7 C. Harb, N. Pokhrel and H. Foroutan, Quantification of the Emission of Atmospheric Microplastics and Nanoplastics via Sea Spray, *Environmental Science & Technology Letters*, 2023, **10**, 513–519.

8 D. B. Shaw, Q. Li, J. K. Nunes and L. Deike, Ocean emission of microplastic, *PNAS Nexus*, 2023, **2**, pgad296.

9 D. Allen, S. Allen, S. Abbasi, A. Baker, M. Bergmann, J. Brahney, T. Butler, R. A. Duce, S. Eckhardt, N. Evangeliou, T. Jickells, M. Kanakidou, P. Kershaw, P. Laj, J. Levermore, D. Li, P. Liss, K. Liu, N. Mahowald, P. Masque, D. Materić, A. G. Mayes, P. McGinnity, I. Osvath, K. A. Prather, J. M. Prospero, L. E. Revell, S. G. Sander, W. J. Shim, J. Slade, A. Stein, O. Tarasova and S. Wright, Microplastics and nanoplastics in the marine-atmosphere environment, *Nature Reviews Earth & Environment*, 2022, **3**, 393–405.

10 C. Wayman and H. Niemann, The fate of plastic in the ocean environment - a minireview, *Environ Sci Process Impacts*, 2021, **23**, 198–212.

11 J. J. Guo, X. P. Huang, L. Xiang, Y. Z. Wang, Y. W. Li, H. Li, Q. Y. Cai, C. H. Mo and M. H. Wong, Source, migration and toxicology of microplastics in soil, *Environ Int*, 2020, **137**, 105263.

12 J. Li, H. Liu and J. Paul Chen, Microplastics in freshwater systems: A review on occurrence, environmental effects, and methods for microplastics detection, *Water Res*, 2018, **137**, 362–374.

13 C. Li, R. Busquets and L. C. Campos, Assessment of microplastics in freshwater systems: A review, *Sci Total Environ*, 2020, **707**, 135578.

14 S. O'Brien, C. Rauert, F. Ribeiro, E. D. Okoffo, S. D. Burrows, J. W. O'Brien, X. Wang, S. L. Wright and K. V. Thomas, There's something in the air: A review of sources, prevalence and behaviour of microplastics in the atmosphere, *Sci Total Environ*, 2023, **874**, 162193.

15 J. Brahney, N. Mahowald, M. Prank, G. Cornwell, Z. Klimont, H. Matsui and K. A. Prather, Constraining the atmospheric limb of the plastic cycle, *Proc Natl Acad Sci U S A*, 2021, **118**, e2020719118.

16 A. Facciola, G. Visalli, M. Pruiti Ciarello and A. Di Pietro, Newly Emerging Airborne Pollutants: Current Knowledge of Health Impact of Micro and Nanoplastics, *Int J Environ Res Public Health*, 2021, **18**, year.

17 A. D. Vethaak and J. Legler, Microplastics and human health, *Science*, 2021, **371**, 672–674.

18 H. A. Leslie, M. J. M. van Velzen, S. H. Brandsma, A. D. Vethaak, J. J. Garcia-Vallejo and M. H. Lamoree, Discovery and quantification of plastic particle pollution in human

blood, *Environ Int*, 2022, **163**, 107199.

19 L. C. Jenner, J. M. Rotchell, R. T. Bennett, M. Cowen, V. Tentzeris and L. R. Sadofsky, Detection of microplastics in human lung tissue using muFTIR spectroscopy, *Sci Total Environ*, 2022, **831**, 154907.

20 E. Can-Güven, Microplastics as emerging atmospheric pollutants: a review and bibliometric analysis, *Air Quality, Atmosphere & Health*, 2020, **14**, 203–215.

21 S. Yang, X. Lu and X. Wang, A Perspective on the Controversy over Global Emission Fluxes of Microplastics from Ocean into the Atmosphere, *Environ Sci Technol*, 2024, **58**, 12304–12312.

22 E. Villermaux, X. Wang and L. Deike, Bubbles spray aerosols: Certitudes and mysteries, *PNAS Nexus*, 2022, **1**, pgac261.

23 L. Deike, B. G. Reichl and F. Paulot, A Mechanistic Sea Spray Generation Function Based on the Sea State and the Physics of Bubble Bursting, *AGU Advances*, 2022, **3**, year.

24 L. Dubitsky, G. B. Deane, D. M. Stokes and J. C. Bird, Modeling the Concentration Enhancement and Selectivity of Plastic Particle Transport in Sea Spray Aerosols, *Journal of Geophysical Research: Oceans*, 2024, **129**, year.

25 B. Ji, A. Singh and J. Feng, Water-to-Air Transfer of Nano/Microsized Particulates: Enrichment Effect in Bubble Bursting Jet Drops, *Nano Lett*, 2022, **22**, 5626–5634.

26 D. C. Blanchard and L. Syzdek, Mechanism for the water-to-air transfer and concentration of bacteria, *Science*, 1970, **170**, 626–8.

27 A. Al Harraq and B. Bharti, Microplastics through the Lens of Colloid Science, *ACS Environ Au*, 2022, **2**, 3–10.

28 M. Kooi, E. H. V. Nes, M. Scheffer and A. A. Koelmans, Ups and Downs in the Ocean: Effects of Biofouling on Vertical Transport of Microplastics, *Environ Sci Technol*, 2017, **51**, 7963–7971.

29 J. W. Scott, K. G. Gunderson, L. A. Green, R. R. Rediske and A. D. Steinman, Perfluoroalkylated Substances (PFAS) Associated with Microplastics in a Lake Environment, *Toxics*, 2021, **9**, year.

30 C. Maddison, C. I. Sathish, D. Lakshmi, O. Wayne and T. Palanisami, An advanced analytical approach to assess the long-term degradation of microplastics in the marine environment, *npj Materials Degradation*, 2023, **7**, year.

31 GESAMP, *Sources, fate and effects of microplastics in the marine environment: a global assessment*, Imo/fao/unescioc/unido/wmo/iaea/un/unep/undp joint group of experts on the scientific aspects of marine environmental protection technical report, 2015.

32 A. Al Harraq, P. J. Brahana, O. Arcemont, D. Zhang, K. T. Valsaraj and B. Bharti, Effects of Weathering on Microplastic Dispersibility and Pollutant Uptake Capacity, *ACS Environ Au*, 2022, **2**, 549–555.

33 M. Aeschlimann, G. Li, Z. A. Kanji and D. M. Mitrano, Microplastics and nanoplastics in the atmosphere: the potential impacts on cloud formation processes, *Nat Geosci*, 2022, **15**, 967–975.

34 Y. Wang, H. Okochi, Y. Tani, H. Hayami, Y. Minami,



- N. Katsumi, M. Takeuchi, A. Sorimachi, Y. Fujii, M. Kajino, K. Adachi, Y. Ishihara, Y. Iwamoto and Y. Niida, Airborne hydrophilic microplastics in cloud water at high altitudes and their role in cloud formation, *Environmental Chemistry Letters*, 2023, **21**, 3055–3062.
- 35 P. Brahana, M. Zhang, E. Nakouzi and B. Bharti, Weathering influences the ice nucleation activity of microplastics, *Nat Commun*, 2024, **15**, 9579.
- 36 P. L. L. Walls, J. C. Bird and J. W. Deming, Enriching particles on a bubble through drainage: Measuring and modeling the concentration of microbial particles in a bubble film at rupture, *Elementa: Science of the Anthropocene*, 2017, **5**, 34.
- 37 L. Dubitsky, O. McRae and J. C. Bird, Enrichment of Scavenged Particles in Jet Drops Determined by Bubble Size and Particle Position, *Phys Rev Lett*, 2023, **130**, 054001.
- 38 S. Yang, T. Zhang, Y. Gan, X. Lu, H. Chen, J. Chen, X. Yang and X. Wang, Constraining Microplastic Particle Emission Flux from the Ocean, *Environmental Science & Technology Letters*, 2022, **9**, 513–519.
- 39 A. I. Catarino, M. C. Leon, Y. Li, S. Lambert, M. Vercauteren, J. Asselman, C. R. Janssen, G. Everaert and M. De Rijcke, Micro- and nanoplastics transfer from seawater to the atmosphere through aerosolization under controlled laboratory conditions, *Mar Pollut Bull*, 2023, **192**, 115015.
- 40 E. R. Kjaergaard, F. Hasager, S. S. Petters, M. Glasius and M. Bilde, Bubble-mediated generation of airborne nanoplastic particles, *Environ Sci Process Impacts*, 2024, **26**, 1216–1226.
- 41 S. Lambert, M. Vercauteren, A. I. Catarino, Y. Li, J. Van Landuyt, N. Boon, G. Everaert, M. De Rijcke, C. R. Janssen and J. Asselman, Aerosolization of micro- and nanoplastics via sea spray: Investigating the role of polymer type, size, and concentration, and potential implications for human exposure, *Environ Pollut*, 2024, **351**, 124105.
- 42 S. Gupta, Bubble floatation, burst, drainage, and droplet release characteristics on a free surface: A review, *Physics of Fluids*, 2023, **35**, 041302.
- 43 H. Wang, Y. Liang, D. Li, R. Chen, X. Yan and H. Zhang, Collisional interaction process between a bubble and particles with different hydrophobicity, *Separation and Purification Technology*, 2022, **301**, year.
- 44 Z. Dai, D. Fornasiero and J. Ralston, Particle-Bubble Attachment in Mineral Flotation, *J Colloid Interface Sci*, 1999, **217**, 70–76.
- 45 Z. Dai, D. Fornasiero and J. Ralston, Particle-bubble collision models—a review, *Adv Colloid Interface Sci*, 2000, **85**, 231–56.
- 46 B. Albijanic, O. Ozdemir, A. V. Nguyen and D. Bradshaw, A review of induction and attachment times of wetting thin films between air bubbles and particles and its relevance in the separation of particles by flotation, *Adv Colloid Interface Sci*, 2010, **159**, 1–21.
- 47 T. Miettinen, J. Ralston and D. Fornasiero, The limits of fine particle flotation, *Minerals Engineering*, 2010, **23**, 420–437.
- 48 P. Sharma, M. Flury and J. Zhou, Detachment of colloids from a solid surface by a moving air-water interface, *J Colloid Interface Sci*, 2008, **326**, 143–50.
- 49 D. C. Blanchard and L. D. Syzdek, Seven problems in bubble and jet drop researches 1, *Limnology and Oceanography*, 1978, **23**, 389–400.
- 50 L. D. Syzdek, Influence of *Serratia marcescens* Pigmentation on Cell Concentrations in Aerosols Produced by Bursting Bubbles, *Appl Environ Microbiol*, 1985, **49**, 173–8.
- 51 S. R. Burger and J. W. Bennett, Droplet enrichment factors of pigmented and nonpigmented *Serratia marcescens*: possible selective function for prodigiosin, *Appl Environ Microbiol*, 1985, **50**, 487–90.
- 52 X. Wang, G. B. Deane, K. A. Moore, O. S. Ryder, M. D. Stokes, C. M. Beall, D. B. Collins, M. V. Santander, S. M. Burrows, C. M. Sultana and K. A. Prather, The role of jet and film drops in controlling the mixing state of submicron sea spray aerosol particles, *Proc Natl Acad Sci U S A*, 2017, **114**, 6978–6983.
- 53 M. Mazzatenta, M. A. Erinin, B. Néel and L. Deike, Linking emitted drops to collective bursting bubbles across a wide range of bubble size distributions, *Journal of Fluid Mechanics*, 2025, **1015**, A8.
- 54 M. D. Stokes, G. B. Deane, K. Prather, T. H. Bertram, M. J. Ruppel, O. S. Ryder, J. M. Brady and D. Zhao, A Marine Aerosol Reference Tank system as a breaking wave analogue for the production of foam and sea-spray aerosols, *Atmospheric Measurement Techniques*, 2013, **6**, 1085–1094.
- 55 X. Jiang, L. Rotily, E. Villermaux and X. Wang, Submicron drops from flapping bursting bubbles, *Proc Natl Acad Sci U S A*, 2022, **119**, e2112924119.
- 56 H. Lhuissier and E. Villermaux, Bursting bubble aerosols, *Journal of Fluid Mechanics*, 2012, **696**, 5–44.
- 57 A. M. Ganan-Calvo, Revision of Bubble Bursting: Universal Scaling Laws of Top Jet Drop Size and Speed, *Phys Rev Lett*, 2017, **119**, 204502.
- 58 C. Harb, J. Pan, S. DeVilbiss, B. Badgley, L. C. Marr, D. G. Schmale, 3rd and H. Foroutan, Increasing Freshwater Salinity Impacts Aerosolized Bacteria, *Environ Sci Technol*, 2021, **55**, 5731–5741.
- 59 C. A. Schneider, W. S. Rasband and K. W. Eliceiri, NIH Image to ImageJ: 25 years of image analysis, *Nat Methods*, 2012, **9**, 671–5.
- 60 L. Dubitsky, M. D. Stokes, G. B. Deane and J. C. Bird, Effects of Salinity Beyond Coalescence on Submicron Aerosol Distributions, *Journal of Geophysical Research: Atmospheres*, 2023, **128**, year.
- 61 J. Mutuku, M. Yanotti, M. Tocock and D. Hatton MacDonald, The Abundance of Microplastics in the World's Oceans: A Systematic Review, *Oceans*, 2024, **5**, 398–428.
- 62 C. Harb and H. Foroutan, A Systematic Analysis of the Salinity Effect on Air Bubbles Evolution: Laboratory Experiments in a Breaking Wave Analog, *Journal of Geophysical Research: Oceans*, 2019, **124**, 7355–7374.
- 63 P. L. Walls, J. C. Bird and L. Bourouiba, Moving with bubbles: a review of the interactions between bubbles and the microorganisms that surround them, *Integr Comp Biol*, 2014, **54**, 1014–25.

64 T.-B. Robinson, H.-A. Giebel and O. Wurl, Riding the Plumes: Characterizing Bubble Scavenging Conditions for the Enrichment of the Sea-Surface Microlayer by Transparent Exopolymer Particles, *Atmosphere*, 2019, **10**, 454.

65 S. I. Karakashev and N. A. Grozev, The Law of Parsimony and the Negative Charge of the Bubbles, *Coatings*, 2020, **10**, 1003.

66 M. Takahashi, Zeta potential of microbubbles in aqueous solutions: electrical properties of the gas-water interface, *J Phys Chem B*, 2005, **109**, 21858–64.

67 D. B. Shaw and L. Deike, Film drop production over a wide range of liquid conditions, *Physical Review Fluids*, 2024, **9**, year.

68 J. Bergfreund, C. Wobill, F. M. Evers, B. Hohermuth, P. Bertsch, L. Lebreton, E. J. Windhab and P. Fischer, Impact of microplastic pollution on breaking waves, *Physics of Fluids*, 2024, **36**, year.

69 Y. Zhang, S. Ding, W. Si, Q. Yin, C. Yang, W. Shi, Y. Xing and X. Gui, Effect of Particle Size and Hydrophobicity on Bubble-Particle Collision Detachment at the Slurry-Foam Phase Interface, *ACS Omega*, 2024, **9**, 4966–4973.

70 S. Vafaei, T. Borca-Tasciuc, M. Z. Podowski, A. Purkayastha, G. Ramanath and P. M. Ajayan, Effect of nanoparticles on sessile droplet contact angle, *Nanotechnology*, 2006, **17**, 2523–7.

71 S. Zhang and X. Han, Effect of different surface modified nanoparticles on viscosity of nanofluids, *Advances in Mechanical Engineering*, 2018, **10**, year.

72 B. P. Binks, Particles as surfactants—similarities and differences, *Current Opinion in Colloid & Interface Science*, 2002, **7**, 21–41.

73 G. Lu, Y.-Y. Duan and X.-D. Wang, Surface tension, viscosity, and rheology of water-based nanofluids: a microscopic interpretation on the molecular level, *Journal of Nanoparticle Research*, 2014, **16**, year.

74 J. Ralston, D. Fornasiero and R. Hayes, Bubble–particle attachment and detachment in flotation, *International Journal of Mineral Processing*, 1999, **56**, 133–164.

75 A. Prajapati, A. Narayan Vaidya and A. R. Kumar, Microplastic properties and their interaction with hydrophobic organic contaminants: a review, *Environ Sci Pollut Res Int*, 2022, **29**, 49490–49512.

76 M. L. A. Kaandorp, D. Lobelle, C. Kehl, H. A. Dijkstra and E. van Sebille, Global mass of buoyant marine plastics dominated by large long-lived debris, *Nature Geoscience*, 2023, **16**, 689–694.

77 S. Zhou, X. Bu, X. Wang, C. Ni, G. Ma, Y. Sun, G. Xie, M. Bilal, M. Alheshibri, A. Hassanzadeh and S. C. Chelgani, Effects of surface roughness on the hydrophilic particles-air bubble attachment, *Journal of Materials Research and Technology*, 2022, **18**, 3884–3893.

78 L. Parkinson and J. Ralston, Dynamic aspects of small bubble and hydrophilic solid encounters, *Adv Colloid Interface Sci*, 2011, **168**, 198–209.

79 D. C. Blanchard and L. D. Syzdek, Water-to-Air Transfer and Enrichment of Bacteria in Drops from Bursting Bubbles, *Appl Environ Microbiol*, 1982, **43**, 1001–5.

80 S. Wangwongwatana, P. V. Scarpino, K. Willeke and P. A. Baron, System for Characterizing Aerosols from Bubbling Liquids, *Aerosol Science and Technology*, 1990, **13**, 297–307.

81 J. A. Quinn, R. A. Steinbrook and J. L. Anderson, Breaking bubbles and the water-to-air transport of particulate matter, *Chemical Engineering Science*, 1975, **30**, 1177–1184.

82 D. C. Blanchard, Jet drop enrichment of bacteria, virus, and dissolved organic material, *pure and applied geophysics*, 1978, **116**, 302–308.

83 D. C. Blanchard, L. D. Syzdek and M. E. Weber, Bubble scavenging of bacteria in freshwater quickly produces bacterial enrichment in airborne jet drops1, *Limnology and Oceanography*, 1981, **26**, 961–964.

84 M. Sakai, A. Tanaka, H. Egawa and G. Sugihara, Enrichment of suspended particles in top jet drops from bursting bubbles, *Journal of Colloid and Interface Science*, 1988, **125**, 428–436.

Data used to plot the figures in this article are available at Figshare at  
<https://doi.org/10.6084/m9.figshare.29906480.v1>.

